Ensemble interactions in strained semiconductor quantum dots

R. Leon
Jet Propulsion Laboratory, California Institute of Technology, Pasadena, CA 91009

S. Marcinkevičius
Department of Physics II – Optics, Royal Institute of Technology, 100 44 Stockholm, Sweden

X. Z. Liao, J. Zou, and D. J. H. Cockayne
Australian Key Centre for Microscopy & Microanalysis, The University of Sydney, Sydney, NSW 2006, Australia.

S. Fafard
Institute for Microstructural Sciences, National Research Council, Ottawa, Ontario, Canada K1A OR6

Large variations in InGaAs quantum dot concentrations were obtained with simultaneous growths on vicinal GaAs [001] substrates with different surface step densities. It was found that decreasing dot-dot separation blue-shifts all levels, narrows intersublevel transition energies, shortens luminescence decay times for excited states, and increases inhomogeneous photoluminescence broadening. These changes in optical properties are attributed to a progressive strain deformation of the confining potentials and to the randomness of increasing dot-dot neighbor interactions.

Successful implementation of technology using self-forming semiconductor quantum dots (QDs) requires a better understanding of their optical properties. Temperature independent [1] Dirac-delta density of states [2] can be exploited in low current threshold lasers [3] and infrared photodetectors [4]. The possibility of using coupled QDs in the fabrication of cellular automata [5] might revolutionize computation technologies, and this is being explored with different epitaxial, molecular and nano-crystalline systems. Recent results have shown 4-fold arrangement in Ge-Si islands [6]. Frequency domain optical storage [7] is an application which exploits the naturally large broadening (inhomogeneous/homogeneous) ratios observed in the photoluminescence (PL) spectra from self-forming QDs. All these device applications need some control and predictability of their opto-electronic properties.

Stranski-Krastanow (S-K) QDs have the advantage of enabling integration with highly developed semiconductor technology. However, some of their idiosyncrasies include interaction with a very stable two-dimensional wetting layer (WL) which is formed at the beginning of the deposition. At a strain dependent critical thickness [8,9] islands begin to form and their concentration increases exponentially with further deposition [10]. The WL can produce an intense peak in the PL spectra from S-K QD structures in low surface densities. Additional complications include strain in the barrier material, in the dot, and randomly varying lateral strain effects from nearby dots. Other recently found complexities particular to InGaAs and GeSi dots are indium or germanium enrichment, internal segregation in the islands [11,12], and differences in ripening behavior [13,14].

Experimental results from energy relaxation processes in QDs have been contradictory. Emission from excited states has been observed from semiconductor dots formed by precipitation [15], S-K growth [16], island induced strain [17] or atomic layer epitaxy [18], these have been explained as phonon bottleneck or phase filling. In a similar manner, several authors have found only ground state emission, even for QDs of larger dimensions, where excited state emission [2, 9,19] is expected. Here we describe the changes in the optical properties of strained self-assembled QDs as a function of concentration. We demonstrate that for intermediate and high surface densities (> $10^9/cm^2$) most of these properties (including the observation of excited states emission) are strongly influenced by dot-dot interactions.

Details of the growth of these samples by MOCVD are reported elsewhere [20]. Different QD densities were obtained by slight variations in substrate miscut angle (θ_m) in [001] GaAs: 0.00°, 0.25°, 0.75°, 1.25° and 2° [all ± 0.25°] towards [110], giving different step densities, which are energetically favorable sites for island nucleation. Simultaneous growths eliminates effects from impurities, contaminants or native defects. Structures grown on $\theta_m = 0.00°$ at the same temperature (550°C) but under conditions producing high surface coverage of stable islands [20] were also investigated. Low temperature (77K) continuous wave (CW) PL spectra were obtained using the 532 nm continuous-wave output of a diode-pumped Nd:YVO_4 for excitation, dispersing the signal with a single grating 0.67 m monochromator, and collecting it with a cooled Ge detector and lock-in techniques. Time-resolved PL measurements were performed at 77 K using a pulsed Ti:sapphire laser (780 nm, 80 fs, 96 MHz) for excitation, and a streak camera, combined with a 0.25 m spectrometer, was used for detection, with temporal

resolution ~ 20 ps. Excitation power ranged from 0.01 to 1 mW and were scaled for different samples in proportion to the QD density to generate the same number of excitons per dot. Island concentrations were measured using atomic force microscopy (AFM) and plan view transmission electron microscopy (TEM). Sizes for the capped QDs were determined with plan-view TEM using a Philips EM430 TEM operating at 300 keV.

Figure 1 shows TEM micrographs of our capped QD structures. Differences in QD average separation are apparent as reported in previous studies [21, 22]. Multi-island strings aligned at multi-atomic step edges are observed here for $\theta_m > 0.75°$. Fig. 2 (a) shows dramatic differences in line-shapes, emission energies, and saturation behavior obtained with the different QD concentrations seen in Fig. 1. QD structures giving spectra labeled A, B and C show similar qualitative behavior, with excited states peaks or "shoulders" appearing at higher excitation. In samples D, E and F, the PL peak from the QDs does not change shape with excitation. However, as seen in Fig. 2. (b), they do exhibit time dependent changes. Fig. 2 (b) shows characteristic time-resolved spectra for two samples with small and large QD density. There is a striking difference between the CW and time-resolved PL spectra for the large density samples: while at the early times after the pulsed excitation the excited state transitions are clearly visible as peaks or shoulders in the time-resolved spectra [Fig. 2 (b)], they are completely missing in the CW mode. One should note, however, that while PL peaks from excited states are seen even at long times after excitation for low QD densities, excited states emission decays more rapidly for densely packed QDs thus giving a much smaller contribution to the time-integrated signal. Figure 3 shows a plot of the energy sub-levels and spacings as a

function of average dot separation (from fits of spectra in Fig. 2) and these are compared with the variation of level energies obtained after post-growth annealing. Table 1 summarizes the experimental observations. These results indicate the following trends with increasing dot-dot proximity: ground states and excited states energies blue shift, intersublevel energy ($\Delta E_{[(i+1)-i]}$) spacings narrow, emission from excited states decays faster and PL emission broadens. It is thus apparent that changing average inter-dot distances strongly affect saturation behavior and energy relaxation in strained quantum dot structures.

A recent report found electron and hole tunneling "in plane" for self assembled quantum dots [23] since these can be in close proximity. Other reports have found red shifts in vertically aligned strained coupled quantum dots [24]. Red shifts would be expected from electronic coupling between dots. Unexpectedly though, one of the most obvious effects reported here is the blue-shifting of all levels. Diminishing dot sizes would explain ground state blue-shifts, however, dot sizes are not observed to change significantly for capped dots. Also, narrower $\Delta E_{[(i+1)-i]}$ are observed as a function of increasing dot concentration (larger $\Delta E_{[(i+1)-i]}$ are calculated for smaller dots).

These results have intriguing similarities with data recently obtained from QDs after post-growth annealing experiments [25,26], where interfacial compositional disordering of the InGaAs/GaAs interface was found to blue-shift all levels while lowering values for $\Delta E_{[(i+1)-i]}$. Comparison of the two sets of experimental results is shown in Fig. 3 and can offer some physical insight. The blue-shifts and narrower $\Delta E_{[(i+1)-i]}$ seen here for denser dot ensembles can be explained by an effective reduction

of the confining potential caused by strain from nearby dots rather than as a consequence of electronic coupling. While no definitive evidence for electronic coupling is obtained from these experiments, it cannot be ruled out, since the faster dynamics of the excited states might be an indication of electronic coupling. Even for the larger inter-dot separations, the near-neighbor distance distribution would allow tunneling between a fraction of the dots. Also, the effective reduction in confinement increases tunneling probability.

Trends towards decreasing PL decay times are seen for increasing dot concentration and for higher eigenstates. The latter observation has also been reported for MBE grown InGaAs dots [27] and dots formed by segregation epitaxy [18]. Recent measurements of PL decay times confirm that reductions in confining potentials associated with interdiffusion shorten PL lifetimes [28]. However, faster inter-level relaxation for dense QD ensembles may be due to several factors. $\Delta E_{[(i+1)-i]}$ is reduced as the QD density increases and approaches GaAs LO phonon energies, potentially changing energy relaxation mechanisms. In addition, close spacing of the QDs might enhance relaxation rates due to level coupling easing inter-dot carrier transfer. One could also expect faster relaxation due to electronic coupling between QDs densely packed in chains [29]. However, we do not observe major differences between the PL dynamics for the high density samples E and F, in one of which the dots are in the chains, and for the other one the dots are distributed randomly (see Fig. 1). This shows that the PL dynamics are more affected by the QD density than by their orientation into closely-spaced chains.

Some of the other spectral features in Fig. 2 can be understood by considering the "bunched" character of the QD. Anisotropic spatial distributions can slightly change

the recombination dynamics in these dots ensembles. The highest concentration found in the first sample set still leaves zones denuded of QDs [see Fig. 1(d, e)] and thus recombination from wetting layer states contributes to the spectra even at low excitation intensities. Enhanced dot-dot interaction will be expected for these "bunched" structures, since most dots are in chains, even for low average QD concentrations. These spectra show some of the effects of dot-dot interactions while still producing an intense WL peak.

Inhomogeneous PL broadening is larger in denser dot ensembles. Dot dimensions and size distributions did not vary significantly from sample to sample. This additional broadening (20-30 meV) in closely spaced dots is most likely due to random spatial variations. Two dots of identical size, shape and ternary composition will then have different emission energies from local strain asymmetries in their confining potential and "disorder-induced" inhomogeneous broadening will be observed. Rapid progress in ordering self assembled QD [30] structures indicates that ordered III-V QD arrays are a possibility for the near future. The possible contribution from larger homogeneous broadening should also be considered In interpreting the causes for the increased inhomogeneous broadening in dense QD ensembles. Further experiments using micro PL (single dot spectroscopy [31]) in differently spaced ordered QD arrays are needed to establish the relative contributions from inhomogeneous and homogeneous broadening.

Thermodynamic stability for S-K islands has been established theoretically [32] and experimentally for InGaAs dots [20] where island in high concentrations were found to be stable against ripening. Interestingly, the morphologically unstable islands (low densities) show better defined 0-D properties. Device applications for these 0-D

structures will then require further studies examining the long term implications of such structural metastability.

In summary, we have shown that varying the average separation in strained semiconductor quantum dots causes radical changes in their optoelectronic properties, and that the randomness of inter-dot spacings adds a significant component to inhomogeneous broadening.

REFERENCES

1. S. Fafard et al., *Surf. Sci.* **361-362**, 778-82 (1996).
2. S. Fafard et al., *Phys Rev B* **50**, R8086 (1994); R. Leon et al., *Science* **267**, 1966 (1995).
3. S. Fafard et al., *Science* **274**, 1350 (1996).
4. J. L. Jimenez et al., *Appl. Phys. Lett.* **71**, 3558 (1997); J. Phillips, K. Kamath, and P. Bhattacharya, *Appl. Phys. Lett.* **72**, 2020 (1998).
5. I. Amlani et al., *Appl. Phys. Lett.* **72**, 2179 (1998).
6. X. Deng and M. Krishnamurthy, *Phys. Rev. Lett.* **81**, (1998).
7. S. Muto, *Jpn. J. Appl. Phys.* **34**, L210 (1995).
8. B. G. Orr et al., *Europhysics Lett.* **19**, 33 (1992).
9. R. Leon et al., *Appl. Phys. Lett.*, **67**, 521 (1995).
10. D. Leonard, K. Pond and P. M. Petroff, *Phys. Rev. B* **50**, 11 687 (1994); R. Leon and S. Fafard, *Phys. Rev. B* **58**, R1726 (1998).
11. X. Z. Liao et al., *Phys. Rev. Lett.* (in press).
12. J. Tersoff, *Phys. Rev. Lett.* **81**, 3183 (1998).
13. F. M. Ross, J. Tersoff, and R. M. Tromp, *Phys. Rev. Lett.* **80**, 984 (1998); G. Medeiros-Ribeiro et al., *Science* **279**, 353 (1998).
14. Y. Kim, B. D. Min, and E. K. Kim, *J. Appl. Phys.* **85**, 2140 (1999).
15. S. A. Empedocles and M. G. Bawendi, *Science* **278**, 2114 (1997).
16. S. Fafard et al., *Phys. Rev. B* **52**, 5752 (1995).
17. H. Lipsanen, M. Sopanen, and J. Ahopelto, *Phys. Rev. B* **51**, 13868 (1995).
18. K. Mukai et al., *Appl. Phys. Lett.* **68**, 3013 (1996).
19. C. Lobo et al., *Appl. Phys. Lett.* **72**, 2850 (1998).
20. R. Leon et al., *Phys. Rev. Lett.* **81**, 2486 (1998).
21. N. Ikoma and S. Ohkouchi, *Jpn. J. Appl. Phys.* **34**, L724 (1995).
22. R. Leon et al., *Phys. Rev. Lett* **78**, 4942 (1997).
23. D. L. Huffaker and D. G. Deppe, Appl. Phys. Lett 73, 366 (1998).
24. G. S. Solomon et al., *Phys. Rev. Lett.* **76**, 952 (1996); M. K. Zundel et al., *Appl. Phys. Lett.* **71**, 2972 (1997).
25. R. Leon et al., *Phys. Rev. B* **58**, R4262, (1998).
26. A notable difference is the variation of the inhomogeneous PL broadening in PL which show opposite trends.
27. S. Raymond et al., *Phys. Rev. B* **54**, 11548 (1996).
28. S. Marcinkevicius and R. Leon, *Phys. Rev. B* **59**, 4630 (1999).
29. A. Tackeuchi et al., *Jpn. J. Appl. Phys* **34** Pt.2, L1439 (1995).
30. R. Notzel et al., *Nature* **392**, 56 (1998); G. Springholz et al, *Science* 282, 734 (1998).
31. L. Landin et al., *Science* **280**, 262 (1998); M. Bayer et al., *Phys. Rev. Lett.* **82**, 1748 (1999).
32. V. A. Shchukin et al., *Phys. Rev. Lett.***75**, 2968 (1995); I. Daruka and A.-L. Barabasi, *Phys. Rev. Lett.* **79**, 3708 (1997); Appl. Phys. Lett. 72, 2102 (1998).

FIGURE CAPTIONS

Fig. 1. Representative images of varying concentrations and spatial arrangements in strained InGaAs/GaAs quantum dots. Imaging conditions were either off-zone-axis or axial bright field. (A) $\theta_m = 0.25 \pm 0.25$, (B) $\theta_m = 0.00 \pm 0.25$, (C) θ_m 0.75 ± 0.25, (D) $\theta_m = 1.25 \pm 0.25$, (E) $\theta_m = 2.00 \pm 0.25$, and (F) $\theta_m = 0.00 \pm 0.25$ (different growth conditions which maximize island coverages).

Fig. 2. (a) 77 K PL spectra of InGaAs QDs with varying concentrations, corresponding to plan view images in Fig. 1. (b) 77 K TRPL spectra, integrated over a 50 ps temporal window with central time values of 100, 840 and 1670 ps after excitation for (i) sample (C), and (ii) sample (E).

Fig. 3. Level energies Vs. average dot-dot separation (red solid diamonds), compared with level shifts induced by thermal intermixing [25] (blue hollow circles).

	QD surface density	Island diam.	$E_{i=0}$	PL decay time (i=0)	$E_{i=1}$	PL decay time (i=1)	$E_{i=2}$	PL decay time (i=2)	$E_{i=3}$	PL decay time (i=3)	2Γ	σ
	cm^{-2}	nm (±5nm)	eV (±0.01)	(ns)	eV	(ns)	eV	(ns)	eV	(ns)	meV	%
A	3.5×10^{8}	24	1.055	____	1.119	____	1.158	_____	1.216	____	37.4	13.4 ± 4.1
B	3.7×10^{8}	25	1.077	5.1	1.126	3.2	1.179	2.1	1.230	0.75	34.6	22 ± 6.1
C	7×10^{8}	23	1.075	1.7	1.129	1.7	1.192	0.98	1.238	0.62	44.7	10.5 ± 2.6
D	2.6×10^{9}	24	1.119	1.4	1.165	1.2	1.213	0.77	1.259	0.56	62	15.4 ± 2.9
E	7.3×10^{9}	25	1.160	2.7	1.198	1.1	1.240	0.62	_____	_____	56	14 ± 3.2
F	2.4×10^{10}	25	1.174	1.8	1.219	1.5	1.270	_____	_____	_____	65	11 ± 2.5

Table 1. Energy levels, intersublevel energy spacings, PL decay times (measured at 80 K), and inhomogeneous broadening (2Γ) for quantum dots with different surface densities. σ was determined from plan view TEM images of QDs, dot concentrations are from AFM of surface dots and plan view TEM of capped dots (shown in Fig. 2). Error bars in $E_{i=0}$ are from local variations in emission from different areas within a QD structure. The error margins for the PL decay times are ± 3%

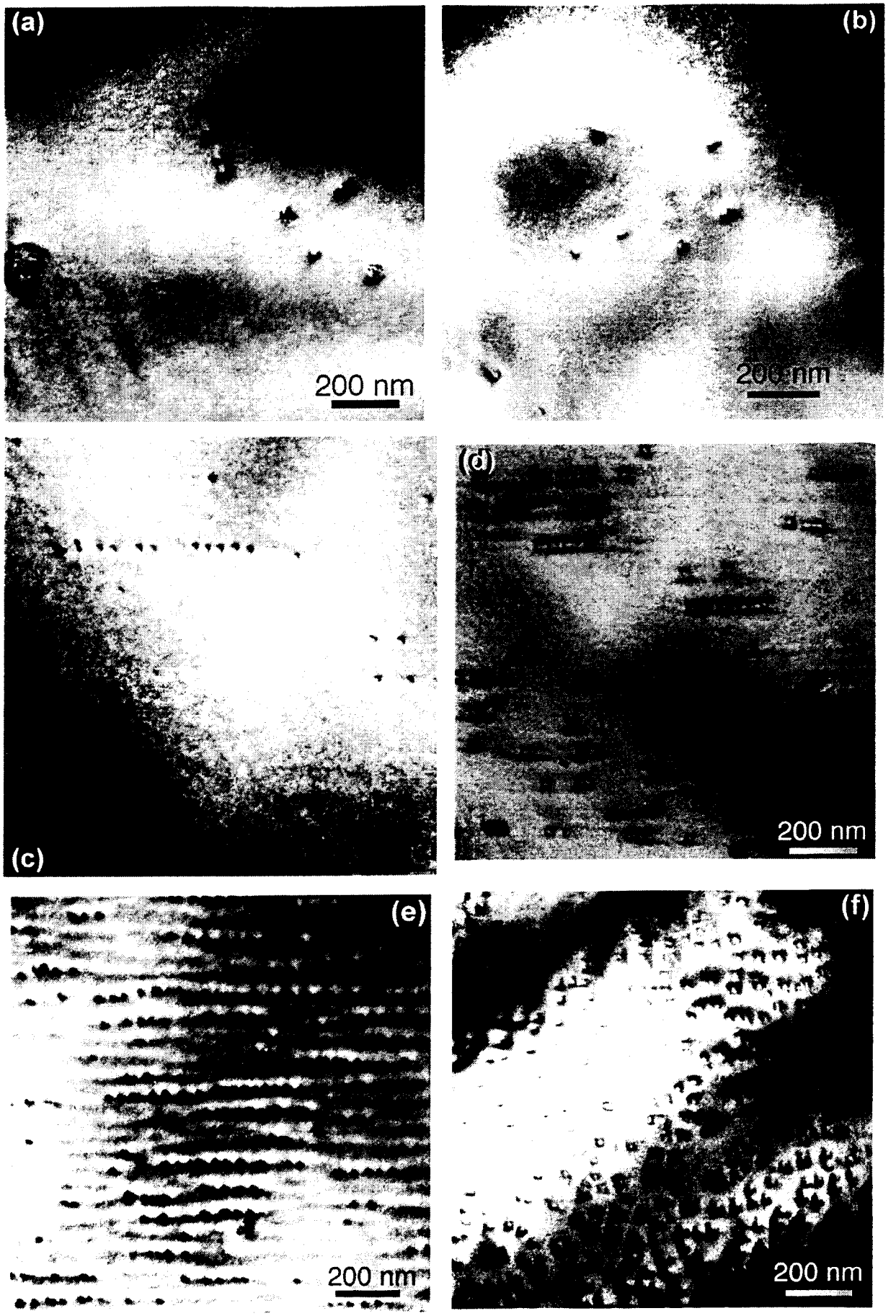
(a)
200 nm
(b)
200 nm
(c)
(d)
200 nm
(e)
200 nm
(f)
200 nm

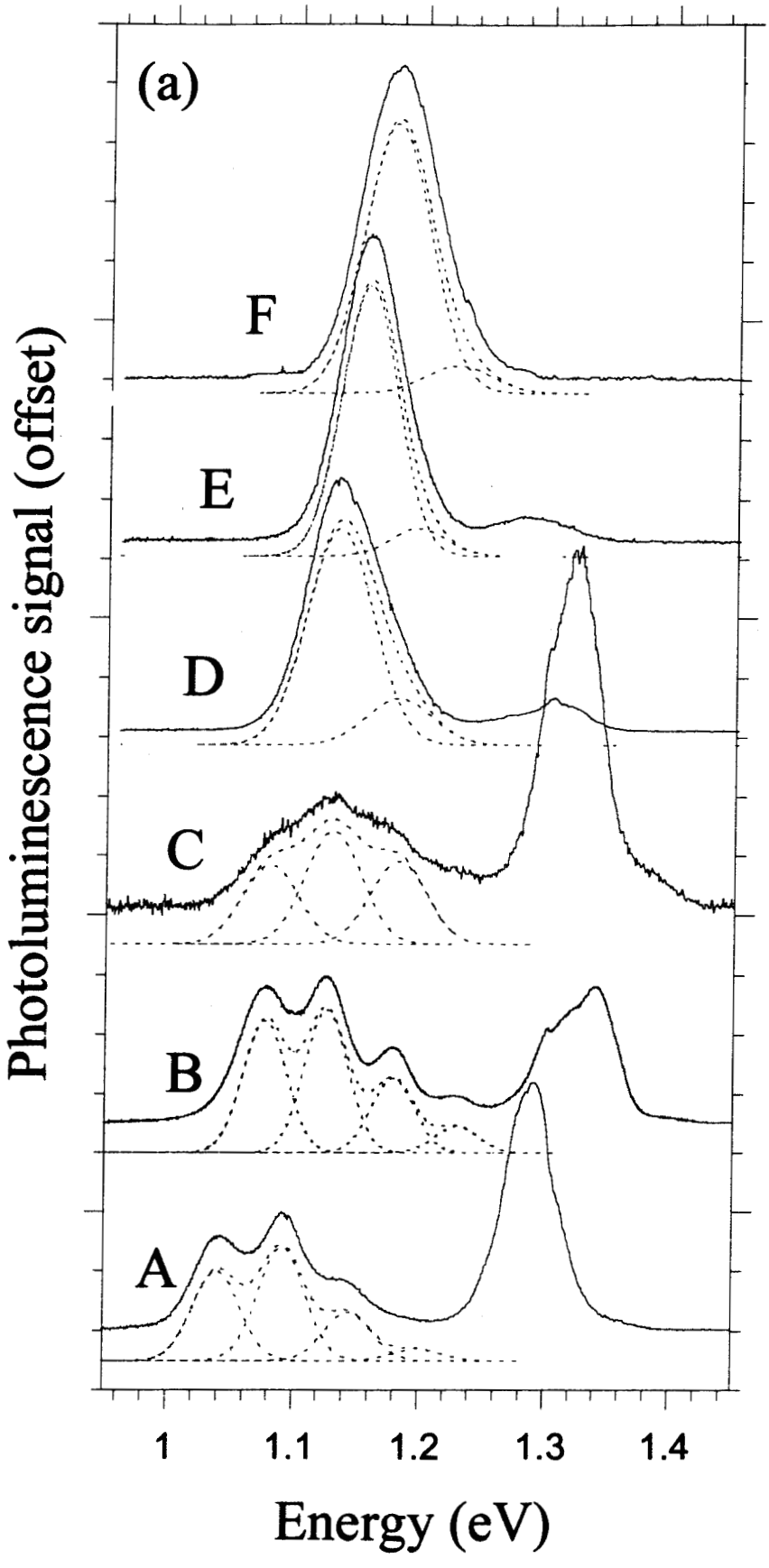
(a)
F
E
D
C
B
A
Photoluminescence signal (offset)
1
1.1
1.2
1.3
1.4
Energy (eV)

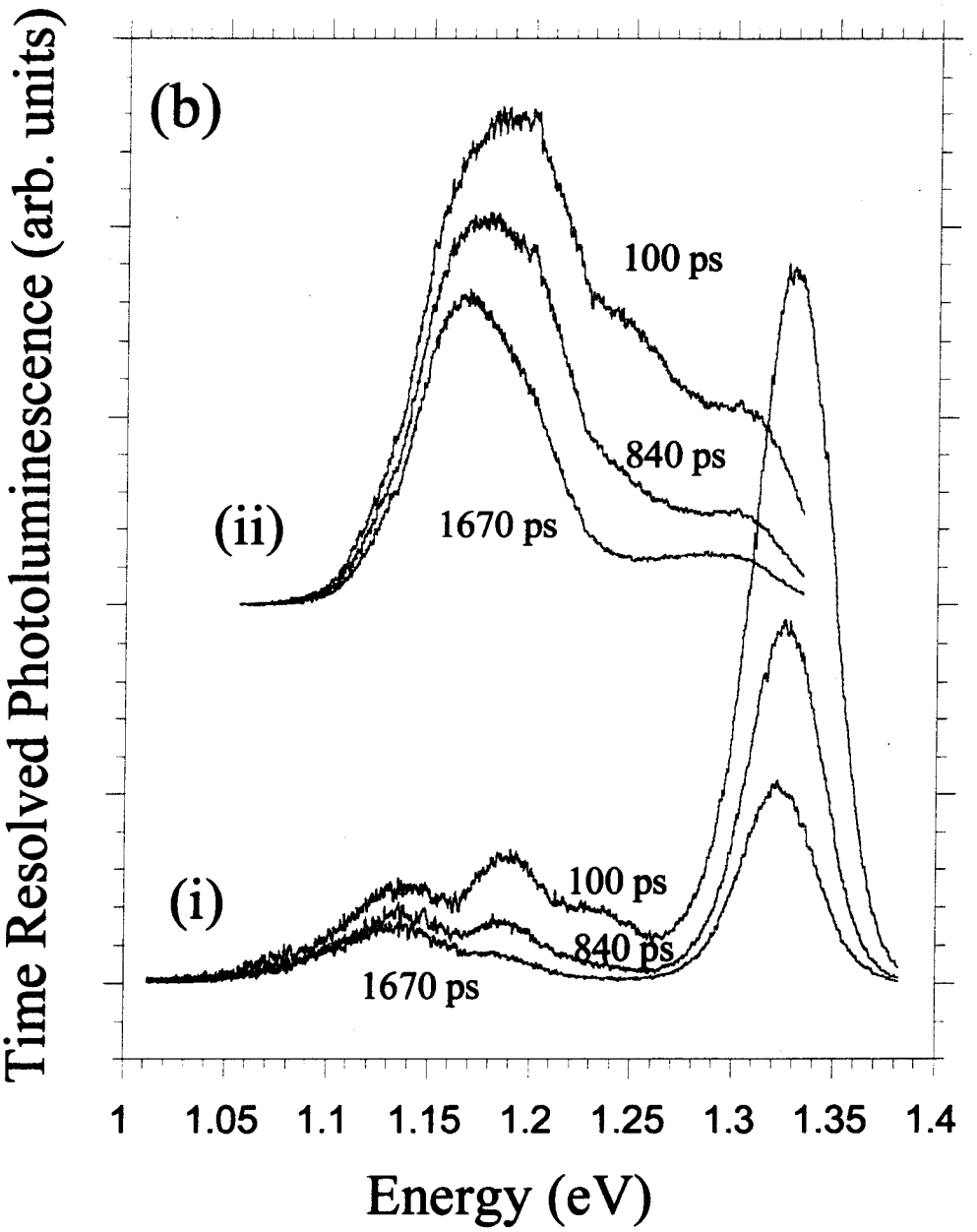
(b)
100 ps
840 ps
1670 ps
(ii)
(i)
100 ps
840 ps
1670 ps
Time Resolved Photoluminescence (arb. units)
1
1.05
1.1
1.15
1.2
1.25
1.3
1.35
1.4
Energy (eV)

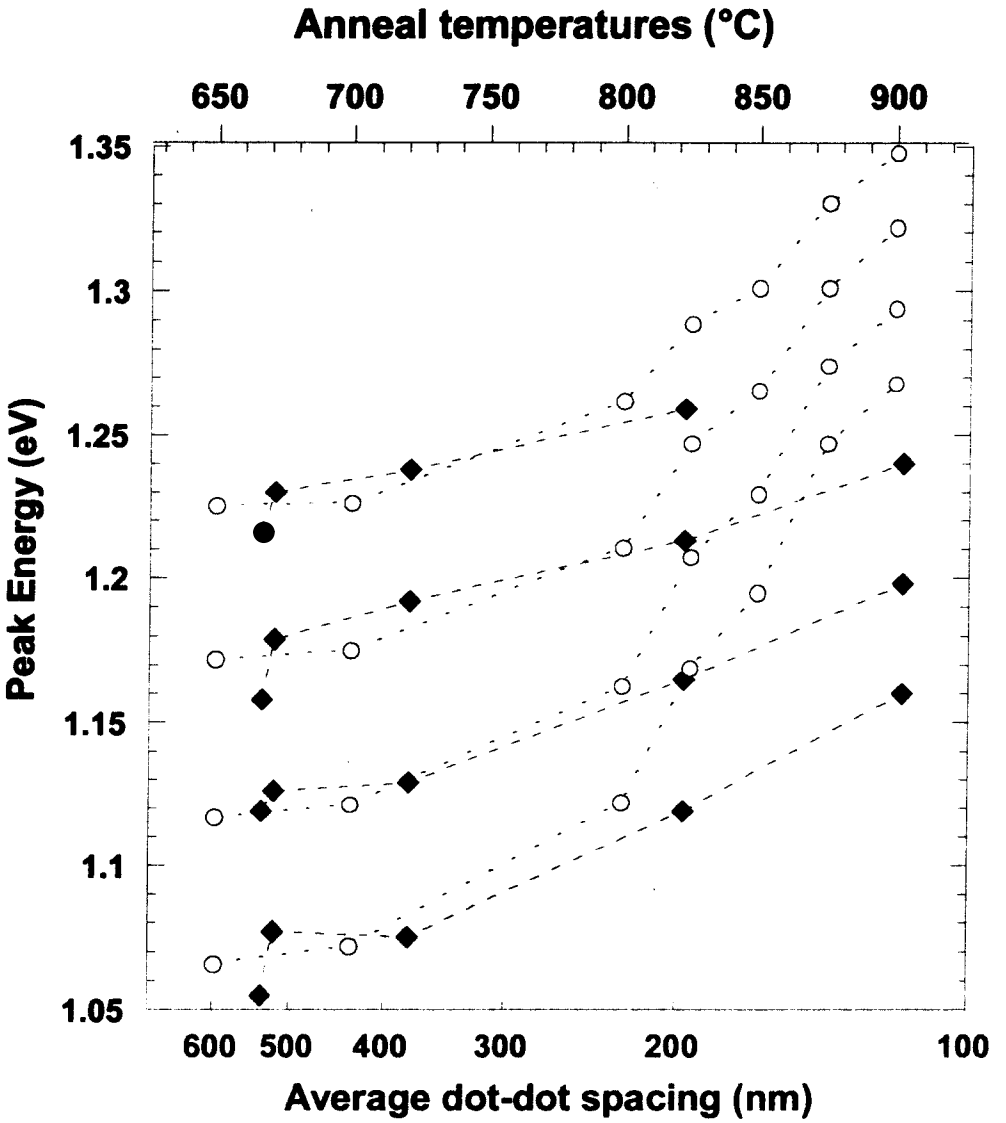
Anneal temperatures (°C)
650
700
750
800
850
900
1.35
1.3
1.25
1.2
1.15
1.1
1.05
Peak Energy (eV)
600
500
400
300
200
100
Average dot-dot spacing (nm)